6684 *Chem. Mater.* **2010,** *22,* 6684–6691
DOI:10.1021/cm102984m

CHEMISTRY OF MATERIALS
Article

Synthesis and Thermodynamically Controlled Anisotropic Assembly of DNA−Silver Nanoprism Conjugates for Diagnostic Applications

Ji-Young Kim and Jae-Seung Lee*

Department of Materials Science and Engineering and Institute for Biomedical Research, Korea University, Anam-dong, Seongbuk-gu, Seoul, Republic of Korea, 136-713

Received October 16, 2010. Revised Manuscript Received November 20, 2010

We have synthesized DNA−silver nanoprism conjugates using the thiol−silver interaction and have assembled them into anisotropic structures with distinctive optical properties simply by controlling thermodynamic conditions. The reversible assembly formation takes advantage of the natural anisotropic architecture of the silver nanoprisms and the cooperative properties of their DNA conjugates. The anisotropic assemblies have been observed not only ex situ by TEM but also in situ in a solution by UV−vis spectroscopy. We have further investigated biodiagnostic applications of the DNA−silver nanoprism conjugates for the colorimetric and quantitative detection of DNA with high selectivity and sensitivity in the full visible range based upon their unique distant-dependent optical properties.

Introduction

Anisotropic silver nanomaterials of different shapes and sizes are an important subject in chemistry, physics, and materials science.[1−7] These materials demonstrate structurally and optically attractive properties in that they are typically nonspherical, range from several nanometers to submicrometers in size, and exhibit strong extinction due to surface plasmon resonance (SPR) that sensitively depends upon their shape and size. Specifically, plate-like triangular silver nanoprisms (AgNPRs), along with other silver anisotropic nanostructures such as rods,[8,9] cubes,[10−12] wires,[8,13] disks,[14−17] and polyhedrons,[18,19] have been extensively investigated with respect to their controlled syntheses and various applications.[3] Importantly, recent synthetic developments for AgNPRs based upon photochemical[5,20] or thermal reactions[21,22] have achieved a very high yield and the systematic and precise control over structural parameters, enabling their fundamental study and versatile application in diagnostics, optics, and electronics.[1,3,23−25] These advances in the synthesis and characterization of AgNPRs have offered substantial opportunities for the synthesis of high quality DNA−silver nanoprism conjugates (DNA-AgNPRs) that would exhibit unique chemical and physical properties not only from AgNPRs and DNA but also from the conjugates themselves, which is analogous to DNA-conjugated isotropic plasmonic nanoparticles such as spherical gold and silver nanoparticles.[26−29] To the best of our knowledge, however,

*Corresponding author. E-mail: jslee79@korea.ac.kr.

(1) Wiley, B. J.; Im, S. H.; Li, Z.-Y.; McLellan, J.; Siekkinen, A.; Xia, Y. *J. Phys. Chem. B* **2006**, *110*, 15666–15675.
(2) Tao, A. R.; Habas, S.; Yang, P. *Small* **2008**, *4*, 310–325.
(3) Millstone, J. E.; Hurst, S. J.; Metraux, G. S.; Cutler, J. I.; Mirkin, C. A. *Small* **2009**, *5*, 646–664.
(4) Murphy, C. J.; Sau, T. K.; Gole, A. M.; Orendorff, C. J.; Gao, J.; Gou, L.; Hunyadi, S. E.; Li, T. *J. Phys. Chem. B* **2005**, *109*, 13857–13870.
(5) Jin, R.; Cao, Y. C.; Hao, E.; Metraux, G. S.; Schatz, G. C.; Mirkin, C. A. *Nature* **2003**, *425*, 487–490.
(6) Sun, Y.; Yin, Y.; Mayers, B.; Herricks, T.; Xia, Y. *Chem. Mater.* **2002**, *14*, 4736–4745.
(7) Xia, Y.; Xiong, Y.; Lim, B.; Skrabalak, S. E. *Angew. Chem., Int. Ed.* **2009**, *48*, 60–103.
(8) Jana, N. R.; Gearheart, L.; Murphy, C. J. *Chem. Commun.* **2001**, 617–618.
(9) Cepak, V. M.; Martin, C. R. *J. Phys. Chem. B* **1998**, *102*, 9985–9990.
(10) Sun, Y.; Xia, T. *Science* **2002**, *298*, 2176–2179.
(11) Im, S. H.; Lee, Y. T.; Wiley, B.; Xia, Y. *Angew. Chem., Int. Ed.* **2005**, *44*, 2154–2157.
(12) Yu, D.; Yam, V. W.-W. *J. Am. Chem. Soc.* **2004**, *126*, 13200–13201.
(13) Sun, Y.; Mayers, B.; Herricks, T.; Xia, Y. *Nano Lett.* **2003**, *3*, 955–960.
(14) Chen, S.; Fan, Z.; Carroll, D. L. *J. Phys. Chem. B* **2002**, *106*, 10777–10781.
(15) Hao, E.; Kelly, K. L.; Hupp, J. T.; Schatz, G. C. *J. Am. Chem. Soc.* **2002**, *124*, 15182–15183.
(16) Maillard, M.; Giorgio, S.; Pileni, M.-P. *J. Phys. Chem. B* **2003**, *107*, 2466–2470.
(17) Guevel, X. L.; Wang, F. Y.; Stranik, O.; Nooney, R.; Gubala, V.; McDonagh, C.; MacCraith, B. D. *J. Phys. Chem. C* **2009**, *113*, 16380–16386.
(18) Tao, A.; Sinsermsuksakul, P.; Yang, P. *Angew. Chem., Int. Ed.* **2006**, *45*, 4597–4601.
(19) Wiley, B.; Herricks, T.; Sun, Y.; Xia, Y. *Nano Lett.* **2004**, *4*, 1733–1739.
(20) Jin, R.; Cao, Y.; Mirkin, C. A.; Kelly, K. L.; Schatz, G. C.; Zheng, J. G. *Science* **2001**, *294*, 1901–1903.
(21) Metraux, G. S.; Mirkin, C. A. *Adv. Mater.* **2005**, *17*, 412–415.
(22) Aherne, D.; Ledwith, D. M.; Gara, M.; Kelly, J. M. *Adv. Funct. Mater.* **2008**, *18*, 2005–2016.
(23) Chen, Y.; Munechika, K.; Ginger, D. S. *Nano Lett.* **2007**, *7*, 690–696.
(24) Sherry, L. J.; Jin, R.; Mirkin, C. A.; Schatz, G. C.; Van Dyune, R. P. *Nano Lett.* **2006**, *6*, 2060–2065.
(25) Metraux, G. S.; Cao, Y. C.; Jin, R.; Mirkin, C. A. *Nano Lett.* **2003**, *3*, 519–522.
(26) Mirkin, C. A.; Letsinger, R. L.; Mucic, R. C.; Storhoff, J. J. *Nature* **1996**, *382*, 607–609.
(27) Jin, R.; Wu, G.; Li, Z.; Mirkin, C. A.; Schatz, G. C. *J. Am. Chem. Soc.* **2003**, *125*, 1643–1654.
(28) Lee, J.-S.; Lytton-Jean, A. K. R.; Hurst, S. J.; Mirkin, C. A. *Nano Lett.* **2007**, *7*, 2112–2115.
(29) Thompson, D. G.; Enright, A.; Faulds, K.; Smith, W. E.; Graham, D. *Anal. Chem.* **2008**, *80*, 2805–2810.

Published on Web 12/06/2010

synthesis of the polyvalent DNA-AgNPRs has not been demonstrated to date, despite the highly developed silver surface chemistry with flat silver surfaces and spherical silver nanoparticles.

Controlled assembly of such anisotropically nanostructured DNA conjugates is another complicated and important issue. In fact, anisotropic nanomaterials as well as isotropic ones are known to exhibit different chemical and physical properties depending upon how they are assembled.[30−32] To date, several methods have been developed to control the assembly formation of anisotropic nanomaterials, such as gold nanorods,[4,33−36] gold nanoprisms,[36,37] silver nanoprisms,[38−40] and silver nanocubes.[41,42] Significantly, these novel assembly structures have provided scope for understanding the specific ways in which assemblies are constructed and have opened up an avenue for their fundamental study and application. These methods, however, usually require selective surface modifications of different facets[37,41] or with different chemicals.[38] In certain cases, the assembly formation of a given nanomaterial is limited to two dimensions on a surface and hardly exhibits anisotropy, despite the highly anisotropic nature of the individual nanoparticles. Recently, Mirkin et al. have demonstrated the concept of inherent shape-directed assembly of triangular gold nanoprisms.[36] Only few studies, however, have yet demonstrated the reversibility of anisotropic assembly formation of anisotropic nanoparticles, which could lead to a variety of applications based upon the unique distance-dependent and assembly structure-dependent optical properties of the same material.

Herein, we report the synthesis of DNA−silver nanoprism conjugates and their thermodynamically controlled anisotropic assemblies in aqueous media. The DNA−silver nanoprism conjugates (DNA-AgNPRs) exhibit the reversible assembly formation of the conjugates based upon the DNA−DNA duplex interconnects and assemble in an anisotropic manner that is controlled by thermodynamic conditions. Importantly, the noncovalently assembled anisotropic structures are observed not only ex situ, by electron microscopy, but also in situ, in a solution using UV−vis spectroscopy, which is strongly indicative of the programmable assembly formation not only by the DNA sequence, nanoparticle size, or simple drying effect, but also by the shape of the nanoparticle.

Experimental Section

Materials. The four HPLC-purified monothiol DNA sequences (**Ag-1**: 5′ HS-A_{10}-ATTATC ACT 3′; **Ag-2**: 5′ HS-A_{10}-AGTGATAAT 3′; **SN-1**: 5′ HS-A_{10}-ATCCTTATCAATATT 3′; **SN-2**: 5′ TAACAATAATCCCTC-A_{10}-SH 3′) and the two unmodified target DNA sequences (**matched**: 5′ GAGGGATTATTGTTAAATATTG**A** TAAGGAT 3′; **mismatched**: 5′ GAGGGATTATTGTTAAATATTG**T**TAAGGAT 3′) were purchased from Genotech (Daejeon, Republic of Korea). Dithiothreitol (DTT, Cat.# 43815), silver nitrate ($AgNO_3$, Cat.# 204390), trisodium citrate dihydrate (Cat.# S4641), sodium borohydride ($NaBH_4$, Cat.# 480886), poly(sodium 4-styrenesulfonate) (PSSS, M_w = 1 000 000, Cat.# 434574), and the chemicals for the buffer preparation were purchased from Sigma-Aldrich (Milwaukee, WI). The NAP-5 sephadex column was purchased from GE Healthcare (Piscataway, NJ). Ultrapure water from a Direct-Q3 system (18.2 MΩ·cm, Millipore; Billerica, MA) was used in this work.

Synthesis of AgNPRs. The aqueous solution of $AgNO_3$ (5 mL, 0.5 mM) was added to the mixture of trisodium citrate (5 mL, 2.5 mM), PSSS (0.25 mL, 500 mg/L), and $NaBH_4$ (0.3 mL, 10 mM, freshly prepared) in water at a rate of 2 mL/min with stirring. A yellow seed solution was obtained in 3 min. Nanoprisms were grown by the injection of aqueous $AgNO_3$ solution (3 mL, 0.5 mM) at a rate of 1 mL/min with vigorous stirring to the mixture of the seed solution (0.02, 0.06, 0.12, and 0.50 mL, for ***XL***, ***L***, ***M***, and ***S***, respectively), pure water (5 mL), and an ascorbic acid solution (0.075 mL, 10 mM). To stabilize the particles, an additional trisodium citrate (0.5 mL, 25 mM) solution was added to each mixture. The average edge length and thickness of the Ag nanoprisms were analyzed by TEM (Tecnai 20, 200 kV, ∼50 prisms per size).

Synthesis of DNA-AgNPRs. Prior to the synthesis of DNA-AgNPRs, excess chemicals were removed from the AgNPR solutions by centrifugation of the nanoprisms (***XL***: 3000 rpm for 30 min; ***L***: 6000 rpm for 20 min; ***M***: 13000 rpm for 10 min; ***S***: 15000 rpm for 20 min), removal of the supernatant, and redispersion of the prisms in 4.4 mM trisodium citrate solution (0.01% Tween 20). The monothiol DNA sequences were deprotected by 0.10 M DTT in phosphate buffer (0.17 M, pH 8.0), purified by a NAP-5 column, and adjusted to 65 μM in water. The DNA was combined with 1 mL of each Ag nanoprism solution (***XL***, ***L***, ***M***, and ***S***), respectively (the final [DNA] = ∼10 μM). The nanoprism solutions were salted (0.15 M NaCl and 0.01% SDS), buffered in 10 mM phosphate at pH 7.4, and incubated at 25 °C for 4 h. The optical properties of DNA-AgNPRs before and after salting were characterized by UV−vis spectroscopy (Agilent 8453 UV−vis spectrophotometer).

Melting Experiments of DNA-AgNPR Assemblies. Four sets of the DNA-AgNPRs (***XL***, ***L***, ***M***, and ***S***) were synthesized, each of which was composed of two complementary conjugates functionalized with **Ag-1** and **Ag-2**, respectively. The two complementary conjugates in each set were combined together for the reversible DNA−DNA hybridization. Melting properties of the hybridized DNA-AgNPRs were analyzed by monitoring the extinction at λ_{MAX}[41] (vide supra) while the temperature was increased from 25 to 65 °C at a rate of 1 °C/min.

Anisotropic Assembly Formation of DNA-AgNPRs. Two sets of DNA-AgNPRs (***XL***), each functionalized with the complementary

(30) Glotzer, S. C.; Solomon, M. J. *Nat. Mater.* **2007**, *6*, 557–562.
(31) Grzelczak, M.; Vermant, J.; Furst, E. M.; Liz-Marzan, L. M. *ACS Nano* **2010**, *4*, 3591–3605.
(32) Baker, J. L.; Widmer-Copper, A.; Toney, M. F.; Geissler, P. L.; Alivisatos, A. P. *Nano Lett.* **2010**, *10*, 195–201.
(33) Wang, L.; Zhu, Y.; Xu, L.; Chen, W.; Kuang, H.; Liu, L.; Agarwal, A.; Xu, C.; Kotov, N. A. *Angew. Chem., Int. Ed.* **2010**, *49*, 5472–5475.
(34) Liu, K.; Nie, Z.; Zhao, N.; Li, W.; Rubinstein, M.; Kumacheva, E. *Science* **2010**, *329*, 197–200.
(35) Nakashima, H.; Furukawa, K.; Kashimura, Y.; Torimitsu, K. *Chem. Commun.* **2007**, 1080–1082.
(36) Jones, M. R.; Macfarlane, R. J.; Lee, B.; Zhang, J.; Young, K. L.; Senesi, A. J.; Senesi, A. J.; Mirkin, C. A. *Nat. Mater.* **2010**, *9*, 913–917.
(37) Millstone, J. E.; Georganopoulou, D. G.; Xu, X.; Wei, W.; Li, S.; Mirkin, C. A. *Small* **2008**, *4*, 2176–2180.
(38) Bae, Y.; Kim, N. H.; Kim, M.; Lee, K. Y.; Han, S. W. *J. Am. Chem. Soc.* **2008**, *130*, 5432–5433.
(39) Zhang, J.; Liu, H.; Zhan, P.; Wang, Z.; Ming, N. *Adv. Funct. Mater.* **2007**, *17*, 1558–1566.
(40) Xue, C.; Li, Z.; Mirkin, C. A. *Small* **2005**, *1*, 513–516.
(41) Rycenga, M.; McLellan, J. M.; Xia, Y. *Adv. Mater.* **2008**, *20*, 2416–2420.
(42) Tao, A.; Sinsermsuksakul, P.; Yang, P. *Nat. Nanotechnol.* **2007**, *2*, 435–440.

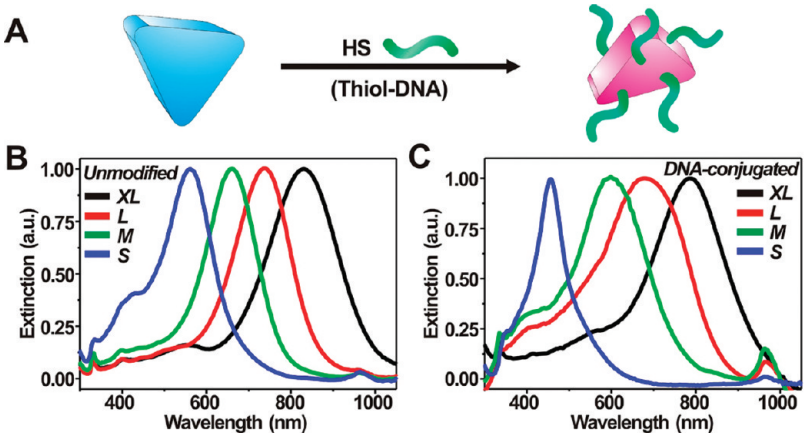

Figure 1. (A) A scheme depicting the conjugation of thiol DNA to a silver nanoprism (AgNPR). (B) UV−vis spectra of unmodified AgNPRs. (C) UV−vis spectra of DNA-conjugated AgNPRs.

thiol-modified DNA sequences (**Ag-1** and **Ag-2**), respectively, were combined and allowed to hybridize (1) at −20 °C and then at 4 °C for 6 h for the edge-to-edge/face assemblies and (2) at 52 °C for 12h and then at 25 °C for 2h for the face-to-face assemblies, respectively. The nanoprism assemblies were characterized by the melting experiments (vide supra) and TEM analysis (Tecnai 20, 200 kV).

Colorimetric Detection of Target Sequences. Two batches of DNA-AgNPR probes (***XL***) were synthesized as described above, each with the two complementary thiol-modified DNA sequences (**SN-1** and **SN-2**), respectively. The DNA-AgNPRs probes were combined with the target DNA strands in a series of concentrations (the final [**matched**] = 1, 5, 10, 25, and 50 nM, respectively) and kept at 25 °C for 12 h to induce DNA-AgNPR assembly formation. The melting experiments were conducted by monitoring the extinction at 785 nm while heating the assembled DNA-AgNPRs from 25 to 65 °C. The melting experiment for the single base-mismatched target sequence ([**mismatched**] = 10 nM) was also performed in the same way.

Results and Discussion

Synthesis of DNA-AgNPRs. For the synthesis of DNA-AgNPRs, plate-like triangular silver nanoprisms of four different sizes were first synthesized following a method previously reported in the literature[22] using poly(sodium 4-styrenesulfonate) (PSSS, M_W = ~1 000 000) as a structure-directing agent, and combined with monothiol DNA (Figure 1A). The mixtures were buffered to 0.15 M NaCl at pH 7.4 (10 mM phosphate), incubated for 4 h, washed by repeated centrifugation, and finally redispersed in a buffer solution. When bare silver nanoprisms were combined with salt ([NaCl] = 0.15 M), the nanostructures completely crashed and formed large aggregates (see Supporting Information, Figure 1S). Once conjugated with DNA, however, no aggregates were observed in the presence of salt, indicative of the efficient conjugation of DNA strands on the silver nanoprism surface, as observed with other analogous DNA−plasmonic nanoparticle conjugates.[26,28] For convenience, we designated the largest DNA-AgNPR as ***XL***, the second largest as ***L***, the third largest as ***M***, and the smallest as ***S***, inspired by their sizes. The optical properties of the bare and DNA-conjugated prisms (***XL***, ***L***, ***M***, and ***S***) were characterized by UV−vis spectroscopy. The four bare prisms (bare ***XL***, ***L***, ***M***, and ***S***) exhibit distinctive primary plasmons at 830, 738, 660, and 561 nm, respectively, where λ_{MAX}[43] increases as the prism edge increases (Figure 1B). When conjugated with DNA, however, these plasmons further blue-shifted by 45−105 nm in wavelength, depending upon the size of the prisms (Figure 1C). Interestingly, we observed that the shift in wavelength was much larger as the prism size decreased. For example, bare ***XL*** has the maximum plasmon at 830 nm, which shifts to 785 nm after the DNA conjugation. This shift of 45 nm for ***XL***, however, increases significantly to 105 nm in the case of ***S*** (from 561 to 456 nm). Based upon this observation, we hypothesized that the relatively small shifts of larger prisms could indicate that the DNA conjugation to larger ones might lead to mainly different dielectric environments on the prism surface due to the DNA monolayer.[24] In contrast, the smaller prisms underwent not only the DNA monolayer formation but also a change in shape and size due to the displacement of the shape-maintaining PSSS on the prism surface by the thiol DNA and oxidative etching by corrosive chloride ion (Cl^-).[19,44]

To confirm the hypothesis regarding the optical and structural changes, we analyzed the bare nanoprisms and DNA conjugates using transmission electron microscopy (TEM) and atomic force microscopy (AFM). In Figure 2A, the four types of bare prisms are identified to be relatively monodispersed but tend to be more truncated as the size decreases. The edge lengths of the bare prisms are determined to be 85.3, 50.0, 39.5, and 16.0 nm for ***XL***, ***L***, ***M***, and ***S***, respectively, and the thickness was 5.08 ± 1.83 nm on average. After the DNA conjugation, ***XL*** shows negligible structural changes except for a slight truncation at the tips (Figure 2B). As the size of the prisms decreases, however, they become rounder and smaller (Figure 2B), indicating the increased truncation and

(43) λ_{MAX} is obtained from the wavelength where the maximum extinction in the visible range takes place.

(44) After we combined DNA and AgNPRs, we also tried the addition of $NaNO_3$ instead of NaCl to the mixture for salting but observed that the nanoprisms crashed, which indicates the thiol DNA strands were rarely conjugated to the prism surface in the absence of Cl^-. We think that Cl^- plays a critical role not only for the oxidative etching but also in the resultant DNA conjugation on the silver nanoprism surface. Further study of this issue is currently underway.

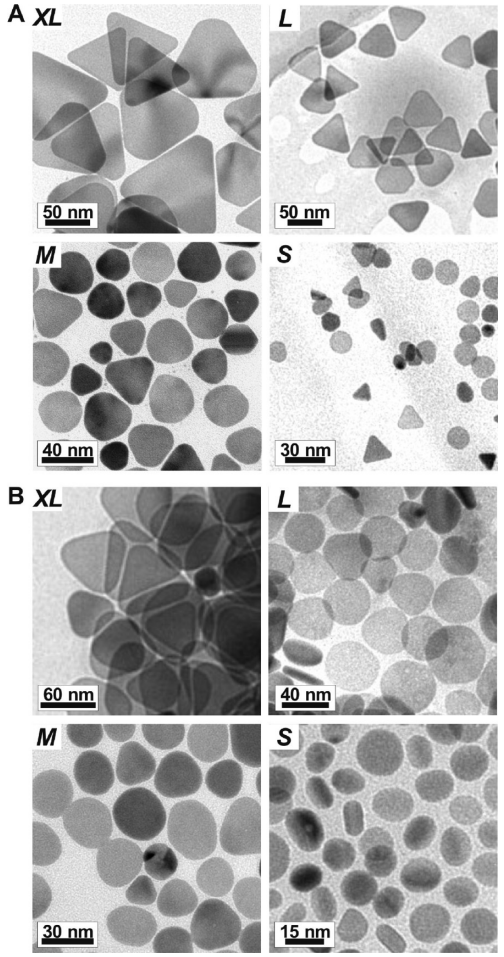

Figure 2. Transmission electron microscopy (TEM) images of (A) unmodified AgNPRs and (B) DNA-conjugated AgNPRs. Note that the nanoprisms are named after their sizes (***XL***, ***L***, ***M***, and ***S***).

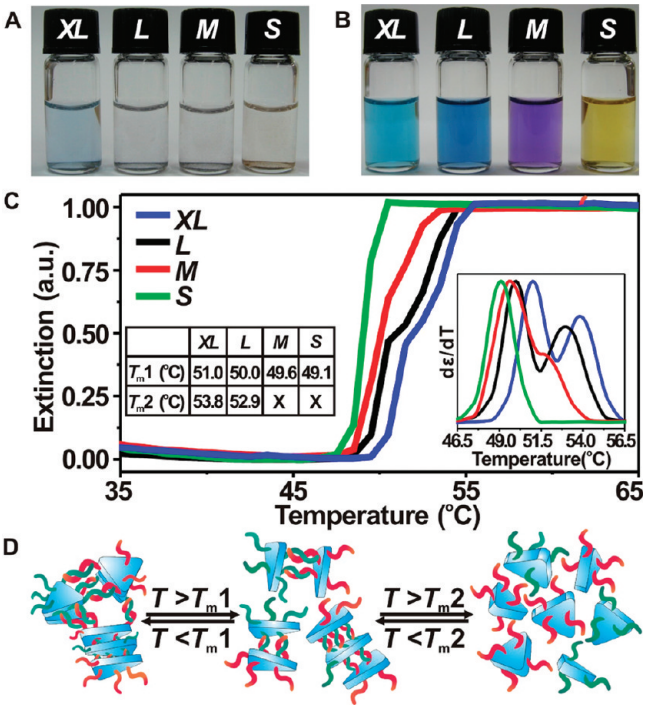

Figure 3. (A) Hybridized DNA-AgNPR solutions. (B) Dehybridized DNA-AgNPR solutions. (C) Melting transitions of hybridized ***XL***, ***L***, ***M***, and ***S***, and their first derivatives (inset). The melting temperatures (T_m's) were obtained from the temperature where the maximum of the first derivative occurs. When there are two local maxima, the lower T_m was labeled as T_m1 and the higher T_m as T_m2. The T_m's for each melting transition are summarized in the inset table. (D) A schematic illustration of the two-phase dehybridization of DNA-AgNPR assemblies. Note that the first dehybridization is associated with the edge-to-edge/face interactions and the second dehybridization with the face-to-face interactions.

structural transformation that lead to the larger spectroscopic changes of smaller prisms in Figure 1C. However, the thickness of the prisms after the conjugation (DNA-AgNPRs) increased only slightly to 7.46 ± 1.47 nm, regardless of the prism edge length. As TEM can "see" only the electron-rich silver nanoprism body of the DNA-AgNPRs and not the surface DNA, we further confirmed the presence of DNA on the prism face by measuring the thickness of the DNA-AgNPRs using AFM. Before the conjugation, the vertical height of a nanoprism was determined to be 5.65 nm by AFM, which is in accordance with the TEM analysis (see Supporting Information, Figure 2S). After conjugation, however, the entire thickness increased to 16.9 nm due to the formation of a DNA monolayer on the prism face. Interestingly, this AFM result suggests that a time period of 4 h is enough for the DNA conjugation on a silver nanoprism face, which is much shorter than the 24 h reported for analogous gold nanoprism systems prepared using cetyltrimethylammonium bromide (CTAB) as a structure-directing reagent.[37]

Reversible and Anisotropic Assembly Properties of DNA-AgNPRs. The dense DNA loading of DNA-AgNPRs was investigated by observing their reversible assembly properties.[27] We first prepared two sets of DNA-AgNPRs, each of which was complementary to the other. These conjugates were well dispersed, exhibited a unique color, and did not form any visible aggregates. When each set was combined together, however, the conjugates rapidly formed very large aggregates in less than half an hour and turned almost colorless as a result of aggregate formation and decreased SPR, indicative of the DNA−DNA interconnect formation between the conjugates, and their unique distance-dependent optical properties (Figure 3A). When heated to 60 °C, however, all of the conjugates disassembled and completely dispersed back, exhibiting their initial colors of light blue, dark blue, violet, and yellow again (Figure 3B). The optical properties of the assembled and dispersed conjugates were characterized by UV−vis spectroscopy (see Supporting Information, Figures 3S and 4S). The reversibility of these assemblies was further characterized by observing their thermal dehybridization using UV−vis spectroscopy to obtain melting transitions. We monitored the extinction of the conjugate mixture solutions at wavelengths where each mixture had the original maximum extinction before the hybridization (λ_{MAX}: 785, 678, 599, and 456 nm for ***XL***, ***L***, ***M***, and ***S***, respectively) as the temperature increased from 25 to 65 °C (Figure 3C). When we consider the transitions below 52 °C, the melting transitions were all very sharp (fwhm of the first derivatives of the melting transitions: ~1.9 °C), suggesting the density of DNA strands on the AgNPR surfaces is high enough to

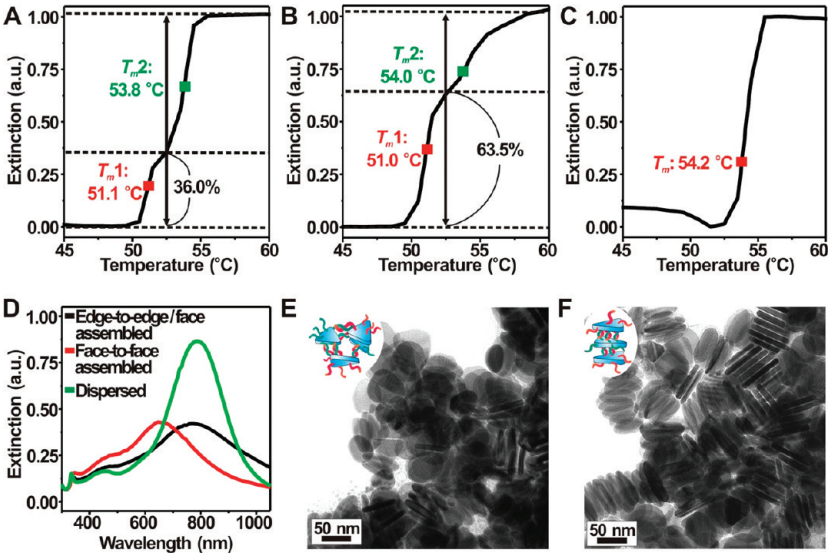

Figure 4. Melting transitions of DNA-AgNPR (***XL***) aggregates assembled (A) at room temperature (25 °C), (B) at −20 °C and then at 4 °C, and (C) at 52 °C. Note that each transition is composed of two phases each occurring at ~51 °C (T_m1) and ~54 °C (T_m2), respectively, but that the portion of each phase differs as the assembly condition changes. (D) UV−vis spectra of dispersed DNA-AgNPRs (***XL***) (green line) and assembled DNA-AgNPRs (***XL***) in an edge-to-edge/face manner (black line) and a face-to-face manner (red line). Both assembled structures exhibit blue-shifts, whose extents depend upon the assembly structures. TEM images of the assembled DNA-AgNPRs (***XL***) in an edge-to-edge/face manner and a face-to-face manner are shown in (E) and (F), respectively, with corresponding schematic illustrations (inset).

exhibit the cooperative melting properties as observed with other DNA-plasmonic nanoparticle conjugates.[27,28,37] The melting temperature (T_m), a midpoint of a melting transition, is notably elevated as the prism size increases (see Figure 3C, inset table). The elevation in T_m of DNA-AgNPRs is obviously due to the increased number of DNA duplex interconnects between the complementary AgNPRs as their surface area increases, leading to an increase in cooperativity and thus T_m.[45] A modeling study was also suggested to theoretically explain the T_m associated with the nanoparticle size.[46]

In addition to the sharp melting transitions due to the dense DNA loading, we further discovered that the typical monotonous melting transition gradually evolved into a stepwise transition as the prism size increased from ***S*** to ***XL***. In Figure 3C, the melting transition of ***S*** exhibits only a single sharp increase at 49.1 °C, similar to those of DNA−spherical gold or silver nanoparticle conjugates. For ***XL***, however, the melting transition is evidently composed of two distinctive phases, whose T_m's are 51.0 °C (T_m1) and 53.8 °C (T_m2), respectively (ΔT_m = ~3 °C). The evolution in the phases of the melting profiles is more clearly illustrated in the inset of Figure 3C, where the first derivatives of the melting transitions divide more distinctively into two peaks as the prism size increases. The presence of the two phases in the melting transitions of DNA-AgNPR aggregates indicates that two types of assembly structures exist concurrently in the system, where the conjugates bind weakly to each other in one type of assembly (T_m1) and strongly in the other (T_m2). To elucidate the origin of the stepwise melting profiles, we reason that the anisotropic structure of a DNA-AgNPR has two types of surfaces: two triangular faces ({111}) and three thin edges.[22] As our nanoprisms are almost equilateral with a constant thickness regardless of the edge length (vide supra), for a given prism both faces are considered to have an identical area as are the three edges. Therefore, we postulate that there are two types of DNA-AgNPR anisotropic assembly structures each based upon (1) face-to-face interactions and (2) edge-to-edge/face interactions. When the two cDNA-AgNPRs are combined, the prisms hybridize to construct both assembly types concurrently at room temperature (25 °C). As the temperature increases, the DNA-AgNPR assemblies based upon the edge-to-edge/face interactions dehybridize at a lower temperature (T_m1) due to the smaller interaction area and the assemblies stacked in the face-to-face manner dehybridize at a higher temperature (T_m2) due to the larger interaction area (Figure 3D), resulting in the two phases of the melting transition in the stepwise manner.

Thermodynamically Controlled Assemblies of DNA-AgNPRs. To verify that the two-phase melting transition stems from the anisotropic nature of the prism assemblies based upon the anisotropic architecture of the AgNPRs, we first hybridized the DNA-AgNPRs (***XL*** and ***L***) with cDNA−spherical gold nanoparticle conjugates (DNA-AuNPs, 15 nm in diameter) and analyzed their melting profiles. In this system, the hybridized DNA-AgNPRs were not expected to effect the anisotropic assembly structure due to the isotropic counterpart (DNA-AuNPs) and would, therefore, result in random or isotropic assembly aggregates from a macroscopic point of view. This hypothesis was verified by obtaining single-phase melting transitions for those assemblies (see Supporting Information, Figure 5S), an indirect proof of the anisotropic assembly formation of the DNA-AgNPRs (***XL***, ***L***), and their resultant T_m's in Figure 3C. This result also

(45) Lee, J.-S.; Stoeva, S. I.; Mirkin, C. A. *J. Am. Chem. Soc.* **2006**, *128*, 8899–8903.
(46) Park, S. Y.; Stroud, D. *Phys. Rev. B* **2003**, *67*, 212202.

explains the effect of the size of the nanoprism and its aspect ratio on the melting transition phase. An aspect ratio is determined as the ratio of the edge length to the thickness.[3] As our prisms and their DNA conjugates have almost identical thickness, regardless of the edge length, smaller nanoprisms have much lower aspect ratios (~3 for ***S***) than larger ones (~17 for ***XL***) and, therefore, are less anisotropic, resulting in single-phase melting transitions similar to those of isotropic nanoparticle assemblies (Figure 3C). Importantly, this observation is a remarkable example of the strong association of the anisotropy of building blocks with the anisotropy of assembly structures.[30]

We further developed our postulation of the thermodynamic control for the assembly of DNA-AgNPRs in an anisotropic manner. According to our postulation, the face-to-face interactions are thermodynamically more favored than the edge-to-edge/face interactions, due to the higher number of the DNA−DNA interconnects between the prisms. At a lower temperature (e.g., 25 °C), however, the chance for edge-to-edge/face interactions is as high as that for face-to-face interactions, because kinetics are more dominant than thermodynamics.[47] Therefore, if we hybridize the DNA-AgNPRs at a temperature (T_{exp}) that is high enough to overcome the kinetically favored edge-to-edge/face hybridization ($T_{exp} > T_m1$) but still below the melting temperature of the face-to-face hybridization ($T_{exp} < T_m2$), we expect only the face-to-face hybridization, leading to the stacked silver nanoprism assembly structures. However, if the DNA-AgNPRs are allowed to hybridize at a low temperature, where both types of hybridizations can begin to take place in a relatively short period of time (< 20 min), a mixture of both structures would be found. The more we decrease the hybridization temperature, the more significant this effect would be, leading to an increased portion of the edge-to-edge/face structures. To confirm this hypothesis we first observed the melting transition of the DNA-AgNPR assemblies hybridized at 25 °C and obtained 36.0% of the first melting phase at 51.1 °C for the disassembly of the edge-to-edge/face hybridization and 64.0% of the second at 53.8 °C for the disassembly of the face-to-face hybridization (Figure 4A). When hybridized abruptly at −20 °C and then at 4 °C for 6 h, the portion of the edge-to-edge/face hybridization dramatically increased to 63.5%, almost twice that at 25 °C, indicating the increased formation of the edge-to-edge/face assemblies (Figure 4B). When hybridized at 52 °C, however, we observed only a single phase transition whose T_m was 54.2 °C, strong evidence of hybridization entirely in the face-to-face manner (Figure 4C). Both assembly structures exhibit distinctive λ_{MAX}'s, one at 655 nm for the face-to-face assembly, and the other at 770 nm for the edge-to-edge/face assembly, which shows a similar shift to the drying-induced self-assemblies of silver nanoprism structures (Figure 4D).[38] In addition to these in situ observations of the assemblies in solution, we further confirmed the anisotropic assembly structures using TEM. Figure 4E shows the assembly structure composed of the randomly oriented individual DNA-AgNPRs hybridized at −20 °C and at 4 °C, which clearly demonstrates that the edge-to-edge/face interactions are dominant under the conditions studied. Figure 4F shows the face-to-face assembly structure consisting of several domains each composed of equally oriented stacked nanoprisms in a face-to-face manner. Significantly, and to the best of our knowledge, this result is the first demonstration of controlling anisotropy of assembly structures simply by changing the temperature of the same system, providing a fundamental concept for the assembly of anisotropic nanobuilding blocks into desired structures using DNA.

Diagnostic Applications of DNA-AgNPRs. Finally, we investigated the versatile diagnostic application of the DNA-AgNPRs by taking advantage of their unique distance-dependent optical properties and programmable assembly properties. In fact, the distance-dependent optical properties of DNA-plasmonic nanoparticle conjugates have been widely utilized for the colorimetric detection of a variety of targets.[29,48−54] Most of them, however, are based upon the SPR of individual gold or silver spherical nanoparticles, whose initial colors are limited to red (Au) or yellow (Ag). To expand the window of the initial colors, our group recently synthesized gold nanoparticle clusters whose optical properties were precisely regulated to exhibit various colors such as red, purple, violet, and blue.[55] In the present study, this diversity of color is significantly expanded with silver nanoprisms whose SPR ranges from the late UV region (~350 nm) to the early NIR region (~900 nm).[22] To demonstrate the versatility of DNA-AgNPRs for the colorimetric detection of oligonucleotide targets, we designed two sets of DNA-AgNPR probes (***XL***), each of which was complementary to each half of the target (Figure 5A). When combined with targets of various concentrations (1, 5, 10, 25, and 50 nM), the probes aggregated and turned almost colorless. As the aggregates were heated, however, they disassembled immediately to turn light blue at certain temperatures depending upon the target concentration. To investigate the quantitative aspect of the detection system, we obtained a series of melting transitions of the DNA-AgNPR aggregates with different target concentrations and plotted the T_m as a function of the target concentration (Figure 5B). The plot of the T_m and the target concentration (Figure 5B, inset) clearly demonstrates an almost linear correlation between them, indicating that this system is highly quantitative for measuring the target concentration. The limit of detection

(47) Park, S. Y.; Lytton-Jean, A. K. R.; Lee, B.; Weigand, S.; Schatz, G. C.; Mirkin, C. A. *Nature* **2008**, *451*, 553–556.
(48) Elghanian, R.; Storhoff, J. J.; Mucic, R. C.; Letsinger, R. L.; Mirkin, C. A. *Science* **1997**, *277*, 1078–1081.
(49) Liu, J.; Lu, Y. *J. Am. Chem. Soc.* **2003**, *125*, 6642–6643.
(50) Han, M. S.; Lytton-Jean, A. K. R.; Oh, B.-K.; Heo, J.; Mirkin, C. A. *Angew. Chem., Int. Ed.* **2006**, *45*, 1807–1810.
(51) Liu, J.; Lu, Y. *Angew. Chem., Int. Ed.* **2006**, *45*, 90–94.
(52) Medley, C. D.; Smith, J. E.; Tang, Z.; Wu, Y.; Tan, W. *Anal. Chem.* **2008**, *80*, 1067–1072.
(53) Xu, W.; Xue, X.; Li, T.; Zeng, H.; Liu, X. *Angew. Chem., Int. Ed.* **2009**, *48*, 6849–6852.
(54) Lee, J.-S.; Han, M. S.; Mirkin, C. A. *Angew. Chem., Int. Ed.* **2007**, *46*, 4093–4096.
(55) Kim, J.-Y.; Lee, J.-S. *Nano Lett.* **2009**, *9*, 4564–4569.

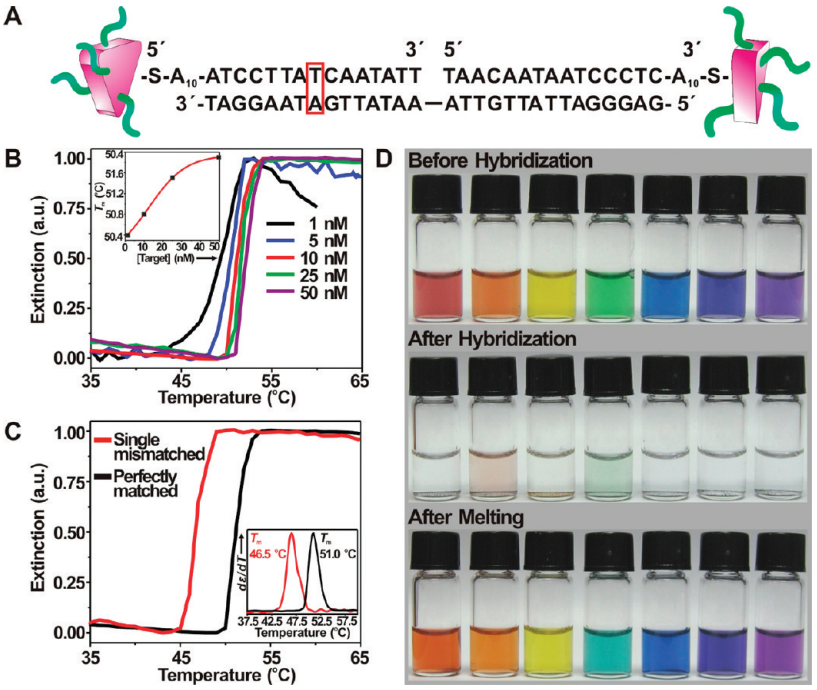

Figure 5. (A) A scheme depicting the design of the colorimetric detection system. One of the target sequence bases is changed from adenine to thymine to examine a single-base mismatch target and is designated in a red box. (B) Melting transitions of DNA-AgNPR (***XL***) aggregates with respect to various target concentrations. The melting temperature (T_m) is plotted as a function of the target concentration (inset). (C) Melting transitions of DNA-AgNPR (***XL***) aggregates formed with a perfectly matched target (black line) and a single-based mismatch target (red line). The first derivatives of melting transitions are shown in the inset. (D) Rainbow colors exhibited by two cDNA-AgNPRs of various sizes before hybridization (top), after hybridization (center), and after melting (bottom).

(LOD) under unoptimized conditions was determined to be 1 nM, comparable to or better than those of other colorimetric DNA detection systems based upon the DNA−plasmonic nanoparticle conjugates.[29,48,55,56] Interestingly, even with ***XL***, we obtained only conventional monotonous melting transitions in this system. This result could be due to the increased interparticle distance (50 bases between prisms compared to 29 bases used for obtaining the two-phase melting transitions) and discontinuous strands in the duplex, leading to orientational flexibility of nanoprisms and thus more disoriented nanoprism assemblies that are associated with averaged single-phase melting transition. We also evaluated whether the detection system could recognize a single-base mismatch of the target sequence by obtaining the melting transitions of the DNA-AgNPR aggregates with the perfectly matched target and the single-base mismatch target, respectively (Figure 5C, each target concentration was 10 nM). The T_m's obtained from the first derivatives of the melting transitions showed a large difference (ΔT_m = ~4.5 °C), which demonstrates the excellent selectivity of the detection system. The most important aspect of this system is its capability to provide full and continuous spectral coverage in the entire visible region by either modulating the size and shape of the nanoprisms or combining two types of nanoprisms with different colors, which is demonstrated in Figure 5D. Before the hybridization of the DNA-AgNPRs, the conjugates exhibited seven initial colors including red, orange, yellow, green, blue, indigo, and violet, or the so-called "rainbow colors" (Figure 5D). These colors turned very pale or almost disappeared after the hybridization of the DNA-AgNPRs because of the reversible DNA-AgNPR assembly formation. Once heated, however, they all disassembled and turned back to the original colors as demonstrated in Figure 5D. When stored at 4 °C at a dark place, the DNA-AgNPRs exhibited the reversible assembly formation without losing the unique optical properties for a month.[57] This completely reversible assembly formation combined with a wide spectral variety in the visible region could serve as a universal platform for nanoparticle-based colorimetric detection schemes, especially for multiple targets that require multiple colors as signals.

Conclusions

We synthesized the DNA−silver nanoprism conjugates and reversibly assembled them in an anisotropic manner by controlling the thermodynamic conditions. Importantly, this is the first synthesis of polyvalent anisotropic silver nanoparticle−DNA conjugates based upon the thiol−silver interactions. These conjugates exhibit various colors in the full visible range, reversible assembly and disassembly properties, and distinctive optical properties dependent upon the assembly structures and interparticle distance. Taken together, it offers a significant chance to expand the design of the anisotropic assembly of nanomaterials and colorimetric detection schemes. Moreover, considering that the in situ characterization

(56) Rosi, N. L.; Mirkin, C. A. *Chem. Rev.* **2005**, *105*, 1547–1562.

(57) Jiang, X.; Zeng, Q.; Yu, A. *Langmuir* **2007**, *23*, 2218–2223.

of nanoparticle assembly is challenging due to the limitations of electron microscopic observation,[31] our work demonstrates an advanced strategy to semiquantitatively analyze anisotropic assembly structures by observing their reversible assembly and disassembly properties. This work reveals a fundamental principle to control the assembly of anisotropic materials based upon the generic cooperative properties of their DNA conjugates, which could be further applied to assemble other anisotropic nanomaterials with various shapes into desired anisotropic structures.[1,4,30]

Acknowledgment. We thank Mr. Jong Bae Park at Korea Basic Science Institute (KBSI, Jeonju, Korea) for his help in the AFM work, and Ms. Semi Park at Korea University for her help in the TEM work. This work was supported by the second stage of the Brain Korea 21 Project in 2010, Basic Science Research Program through the National Research Foundation of Korea (NRF) funded by the Ministry of Education, Science and Technology (Grant No. 2009-0089572), and Seoul R&BD Program (Grant No. ST090795).

Supporting Information Available: Materials, experimental details for the synthesis of the DNA-AgNPRs, UV−vis spectroscopy analysis, melting experiments of assembled DNA-AgNPRs, TEM analysis, and the colorimetric detection of target sequences (PDF). This material is available free of charge via the Internet at http://pubs.acs.org.